Study of the sorption and acidic properties of MTW-type zeolite

B.H. Chiche, R. Dutartre, F. Di Renzo, F. Fajula [1]

Laboratoire de Matériaux Catalytiques et Catalyse en Chimie Organique, URA 418 CNRS, ENSCM, 8 rue de l'Ecole Normale, 34053 Montpellier Cedex, France

A. Katovic, A. Regina and G. Giordano

Dipartimento di Ingegneria Chimica e dei Materiali, Università della Calabria, I-87100 Rende, Italy

Received 10 January 1995; accepted 18 January 1995

The acidity of H-MTW-type zeolite has been investigated using infrared spectroscopy of adsorbed pyridine. Pore volume has been measured by nitrogen and *n*-hexane adsorption. The zeolite exhibits infrared signals at 3612 and 3580 cm^{-1} tentatively attributed to bridging hydroxyl groups vibrating in the main channel and in the six-membered rings of the structure, respectively. Both hydroxyl groups possess high acid strength and are readily accessible to pyridine. H-MTW shows a *n*-hexane cracking activity at 350°C comparable to that obtained with MFI and BEA-type materials with a product selectivity between medium and large pore structural types.

Keywords: zeolite; MTW; ZSM-12; acidity; pyridine adsorption; FTIR; *n*-hexane cracking

1. Introduction

Zeolites with the MTW structure, such as ZSM-12, TEA silicate, CZH-5, Nu-13 and TPZ-2 [1,2], have potential for applications in catalysis due to their unidirectional twelve-membered ring linear channel system with apertures of 5.6 × 7.7 Å. The synthesis of this type of material has been disclosed first in 1974 [3] and has been described since then in a series of literature papers [4–7]. A variety of organic molecules, including alkylammonium ions, alkylamines and nitrogen-containing polymers direct the crystallization of MTW type zeolites [8], but the most commonly used are tetraethyl and methyltriethylammonium cations, TEA and MTEA, respectively. A better efficiency for the incorporation of aluminium in the framework was found when MTEA was used as template [9].

[1] To whom correspondence should be addressed.

The literature also reports ^{29}Si NMR studies of the MTW structure performed on highly siliceous samples [10], but little information is, however, available regarding the sorption and acidic properties of activated MTW-type zeolites. Since both properties are of particular relevance for catalytic applications, we have undertaken the present study with the aim of a better knowledge of these materials. Pyridine adsorption was followed using infrared spectroscopy in order to characterize the nature and the accessibility of the acid sites and *n*-hexane cracking was performed to evaluate catalytic activity.

2. Experimental

A highly crystalline sample of ZSM-12 has been synthesized by crystallization for 8 days at 140°C under static conditions of a gel having the composition: $5Na_2O$–10MTEABr–$1.25Al_2O_3$–$50SiO_2$–$1000H_2O$. The details of the gel preparation procedure and the main characteristics of the parent zeolite are given elsewhere [7,9]. The protonic form was obtained after overnight calcination in flowing dry air at 600°C followed by two ion exchange treatments in 1 M ammonium chloride solution (100 ml/g of zeolite) and a final calcination in air at 550°C.

The activated zeolite was characterized by X-ray diffraction (XRD, CGR theta 60), ^{27}Al NMR spectroscopy (AMX 400 Bruker, 104.2 MHz), scanning electron microscopy (SEM, Stereoscan Cambridge 360) and Fourier transform infrared spectroscopy (FTIR, Nicolet 320).

Nitrogen adsorption–desorption isotherms were determined using an automated porosimeter (Micromeritics Asap 2000). *n*-hexane sorption capacity at room temperature and a relative pressure P/P_0 of 0.15 was measured by gravimetry (Setaram B 85 Balance) assuming normal liquid density of the adsorbed phase. The acidity was probed using pyridine adsorption and infrared spectroscopy as described recently in detail [11]. The catalytic activity was evaluated for *n*-hexane cracking at 350°C and atmospheric pressure with a nitrogen to hydrocarbon ratio of 17 and a space velocity (WHSV) of 2 h^{-1}. The cracking test results have been compared to those obtained with H-beta (BEA-type, Si/Al = 23, crystal size 0.4 μm) and H-ZSM-5 (MFI-type, Si/Al = 17, crystal size 1 μm).

3. Results and discussion

Table 1 reports the main characteristics of the zeolite sample after its transformation into the protonic form. The observed Si/Al ratio corresponded to an aluminium content of 0.6 atoms per unit cell. ^{27}Al MAS NMR spectroscopy revealed that above 90% of the aluminium atoms were tetrahedrally coordinated (fig. 1). The final composition of the sample was therefore close to that of the synthesis gel indicating an efficient incorporation of aluminium in the framework as already dis-

Table 1
Main physicochemical characteristics of H-ZSM-12

Composition (molar ratios)		Size (μm)	Morphology	Microporous volume (ml/g)	
Si/Al	Na/Al			N_2	*n*-hexane
23	0.12	1	rice-like crystals	0.095	0.070

cussed previously [8,9]. A small amount of sodium ions (0.07 per unit cell) was not exchanged with the activation procedure we followed.

The adsorption–desorption isotherm for nitrogen, shown in fig. 2, indicated that, besides the adsorption in micropores, amounting to a volume of 0.095 ml/g, there was a significant contribution of adsorption on the external surface of the grains and in mesopores (0.11 ml/g). Such features are well in line with the SEM observations of the crystals, which appeared as rice-shaped particles with an average size of 1 μm and irregular rough surface. As shown in table 1, the microporous volume accessible to *n*-hexane at room temperature represented 75% of the one accessible to nitrogen. The observed sorption capacities actually corresponded to those expected for zeolites of the MTW group [3,8].

The infrared spectrum of the hydroxyl stretching region (3800–3300 cm^{-1}) after outgassing the zeolite wafer at 450°C under vacuum, exhibited five signals (fig. 3a) at 3780, 3747, 3667, 3612 and 3580 cm^{-1}. By analogy with what is known for other zeolite types we can ascribe the signals at 3780 and 3667 cm^{-1} to hydroxyl groups bound to extraframework (dislodged or partially attached) aluminium containing species, the signal at 3747 cm^{-1} to isolated silanol groups and the signal at 3612 cm^{-1} to structural acidic Al–OH–Si groups [12–14]. The peak at 3580 cm^{-1} originated probably from structural bridging OH groups vibrating in small (six- or eight-membered) rings. The latter situation is indeed known [15] to induce a bathochromic shift with respect to the unperturbed position as a result of

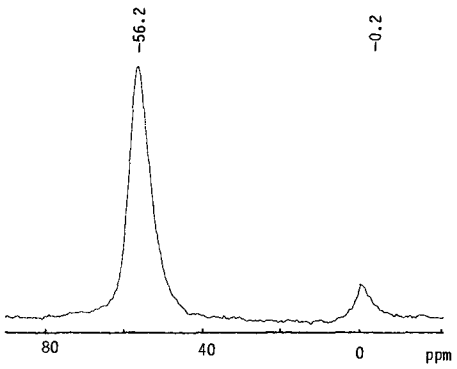

Fig. 1. ^{27}Al MAS NMR spectrum of H-ZSM-12 at 104.2 MHz (0.8 μs for π/20 pulse width, delay time 1 s, spinning rate 12 kHz).

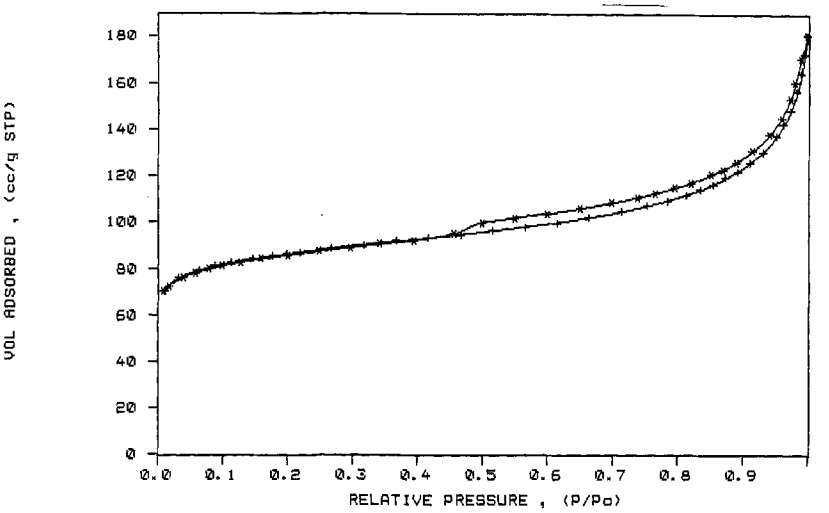

Fig. 2. Adsorption–desorption isotherm for nitrogen at 77 K.

an electrostatic interaction with the oxygen atoms. In the MTW structure, the large twelve-membered rings that delineate the main channels are only composed of six-membered rings. Framework hydroxyl groups pointing towards the main channel and the six-rings could account therefore for the signals at 3612 and 3580 cm^{-1}, respectively. The small amounts of extraframework species found by NMR could hardly account for an infrared signal of such an intensity and support its assignment to a structural hydroxyl. As regards implications for acidity, it is important to stress that all the aluminium-containing species present in the structure were acidic and accessible to pyridine. As shown by fig. 3b, adsorption of the base at 150°C followed by evacuation led to the total disappearance of all signals, with the exception of the non-acidic silanol groups, which were nevertheless perturbed by the adsorbed molecule [11,12]. The fact that the signal at 3580 cm^{-1} also vanished suggests, if the hypothesis developed above is correct, that the location of the proton in a restrained environment does not prevent its full transfer to the base. Fig. 3b also shows the two signals characteristic of pyridinium ions at 3265 and 3180 cm^{-1}, in the region of the aromatic C–H and N–H vibrations, and a broad signal in the range 3200–2400 cm^{-1} due to hydroxyl groups hydrogen-bonded to the aromatic ring.

In the region of the ring vibration signals fig. 4a is typical of the formation of pyridinium ions on Brønsted sites, at 1635 and 1546 cm^{-1} (8a and 19b modes, respectively), of pyridine coordinated to Lewis centres, at 1622 and 1455 cm^{-1} and of labile hydrogen-bonded or sodium-bonded species, at 1597, 1446 and 1427 cm^{-1} were detected. The 19b vibrational mode of the pyridine ring at 1490 cm^{-1} is common to all types of adsorbed species. An evacuation of the sample for 2 h at 300°C removed the labile species (fig. 4b) but had little influence on the pyridine molecules interacting with Brønsted and Lewis sites. In the region of the OH

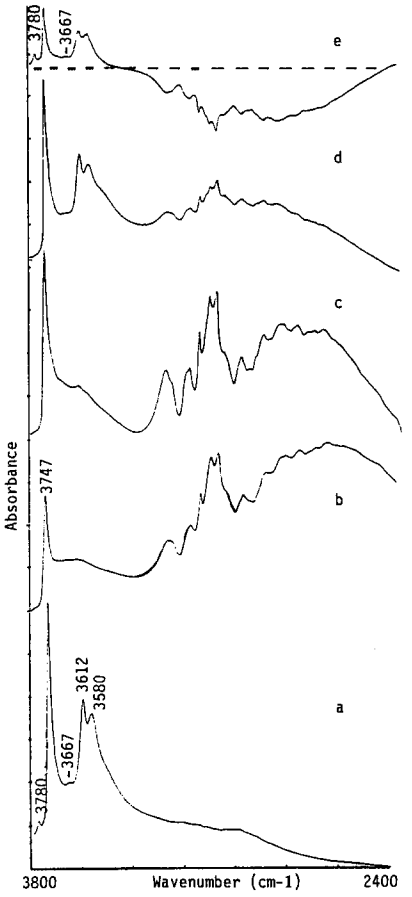

Fig. 3. Infrared spectra of H-ZSM-12. (a) Starting material outgassed at 450°C, (b) after adsorption of pyridine at 150°C and desorption at 150°C, (c) after desorption at 300°C, (d) after desorption at 450°C, (e) difference spectrum (a) – (d).

stretching vibrations, a net increase of the intensity of the signal of the silanol groups was observed, due to the removal of pyridine adsorbed on the surface by hydrogen bonding, and some hydroxyls vibrating at 3612 cm^{-1} were regenerated (fig. 3c). A further desorption treatment performed at a temperature of 450°C (fig. 3d), allowed the recovery of approximately 60% of the intensity of the signals at 3612 and 3580 cm^{-1} while the signals at 3780 and 3667 cm^{-1} remained unobservable. In the 1700–1400 cm^{-1} region (fig. 4c), the signals characteristic of the pyridinium ions decreased and a new band, at 1462 cm^{-1} appeared. This latter signal, also reported for various zeolite types after desorption of pyridine by high-temperature treatment, has been identified as a C–H bending vibration mode in inium ions formed by a nucleophilic attack by a lattice oxygen followed by protonation of pyridine molecules adsorbed on Lewis sites [11]. The formation of inium ions requires the presence of strong Lewis/Brønsted pairs of sites and makes difficult a

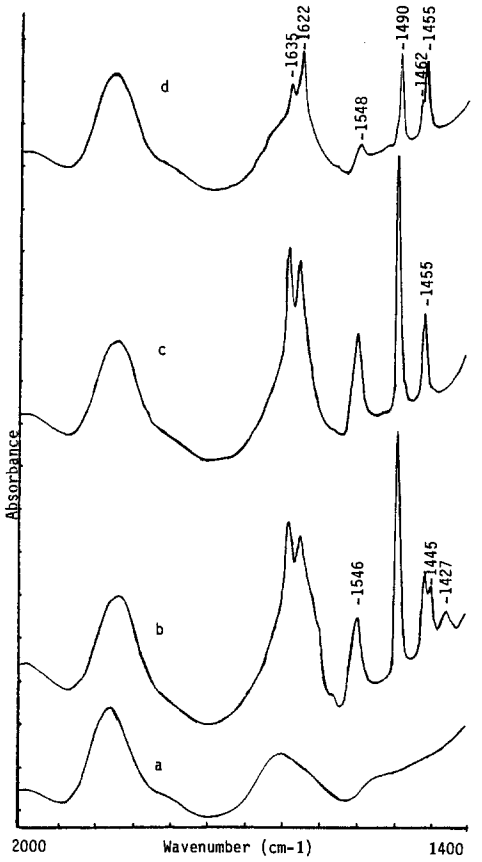

Fig. 4. Infrared spectra of pyridine adsorbed on H-ZSM-12. (a) Starting material outgassed at 450°C, (b) after adsorption of pyridine at 150°C and desorption at 150°C, (c) after desorption at 300°C, (d) after desorption at 450°C.

quantitative analysis of the spectrum in terms of relative amounts of Lewis and Brønsted sites still retaining pyridine after desorption at 450°C. The difference spectrum, shown in fig. 3e, indicated nevertheless clearly that all the hydroxyls, including some silanol groups, interacted directly or indirectly with pyridine under these conditions. Evidence for indirect interaction (perturbation of silanol groups by pyridine coordinated on Lewis acid centres [11,16,17] or pyridinium ions) was provided by the broad (negative) signal centered around 2900 cm^{-1} in the difference spectrum.

Finally, the estimation of the relative amount of pyridine left on the surface after outgassing at 450°C could be made from the intensity of the signal at 1490 cm^{-1}, which is common to both types of acidities, as said before. This led to the conclusion that nearly 30% of the original amount of base had not been desorbed at 450°C and indicated the presence of sites with high acid strength.

Table 2
Pore dimensions, activity and selectivity ratios in *n*-hexane cracking for three different zeolite types

	Structure type		
	MFI	MTW	BEA
pore size (Å)	5.5 × 5.6	5.6 × 7.7	6.4 × 7.6
Si/Al	17	23	23
k (g g^{-1} h^{-1})	0.45	0.37	0.52
isoC$_4$/nC$_4$	0.5	1.2	2.5
isoC$_5$/nC$_5$	0.5	1.1	2.5

The *n*-hexane cracking experiments confirmed the strong acidity of the zeolite and revealed good stability as a function of time. Under the conditions of our measurements an initial conversion of 17% was obtained. The cracking activity developed by the H-ZSM-12 sample, expressed as the apparent first order rate constant ($k = -\text{WSHV}\ \ln(1\text{-}x)$, where x is the conversion), was comparable to the ones observed with the H-ZSM-5 and H-beta zeolite samples used in reference runs (table 2). After 2 h on stream the activity loss was 20% for H-ZSM-12 and H-ZSM-5 and 80% for H-beta. The product distribution was barely modified by deactivation and showed (table 2) that the selectivity ratio of branched to normal paraffins was directly correlated with the size of the pore openings of the structure. The observed values fell between those found for ZSM-5 and zeolite beta, which are representative of medium and large pore structures, respectively, in agreement with the findings of Weitkamp et al. [18] and Martens et al. [19], who used the hydrocracking of C$_{10}$-naphthenes and *n*-decane as catalytic tests, respectively.

4. Conclusions

The thermal and ion-exchange treatments performed during the activation step generate minor amounts of extraframework species which do not reduce the sorption capacity of the zeolite. The microporous volume available to nitrogen equals 0.095 ml/g, 75% of each being accessible to *n*-hexane. All the aluminium containing species present in the material show a strong acidic character and are readily reached and neutralized by the pyridine molecule. The *n*-hexane cracking activity developed by MTW-type zeolite is comparable to that of MFI- and BEA-type zeolites of similar aluminium contents. The selectivity, with respect to the formation of branched hydrocarbons, is consistent with the size of the pore openings and ranks MTW-type zeolites between medium and large pore structural types. Further infrared studies using weaker bases as probe molecules, such as carbon monoxide or ethylene for example, should provide more details on the strength of the acid sites and fully elucidate the fate of the hydroxyl group responsible for the 3580 cm^{-1} signal.

Acknowledgement

Part of this work has been conducted under the frame of a joint CNRS/CNR French–Italian project.

References

[1] E.M. Meier and D.H. Olson, *Atlas of Zeolite Structure Types*, 3rd rev. Ed. (Butterworth-Heinemann, London, 1992).
[2] R.B. Lapierre, A.C. Rohrman Jr., J.L. Schlenker, J.D. Wood, M.K. Rubin and W.J. Rohrbaugh, Zeolites 5 (1985) 346.
[3] E.J. Rosinski and M.K. Rubin, US Patent 3,832,449 (1974).
[4] S. Ernst, P.A. Jacobs, J.A. Martens and J. Weitkamp, Zeolites 7 (1987) 458.
[5] X. Shou-He and L. Hexuan, *Preprints of Posters 7th Int. Zeolite Association* (Japan Association of Zeolites, Tokyo, 1986) p. 25.
[6] F. Di Renzo, A. Albizane, M.A. Nicolle, F. Fajula, F. Figueras and T. Des Courières, Stud. Surf. Sci. Catal. 65 (1991) 603.
[7] A. Katovic and G. Giordano, Chem. Express 6 (1991) 969.
[8] P.A. Jacobs and J.A. Martens, Stud. Surf. Sci. Catal. 33 (1987) 297.
[9] A. Katovic and G. Giordano, ACS Spring Meeting, Anaheim 1995, submitted.
[10] C.A. Fyfe, H. Strobl, G.T. Kokotailo, C.T. Pasztor, G.E. Barlow and S. Bradley, Zeolites 8 (1988) 132.
[11] B.H. Chiche, F. Fajula and E. Garrone, J. Catal. 146 (1994) 460.
[12] J.W. Ward, J. Phys. Chem. 73 (1969) 2086.
[13] E. Bourgeat-Lami, P. Massiani, F. Di Renzo, P. Espiau, F. Fajula and T. Des Courières, Appl. Catal. 72 (1991) 139.
[14] E. Loeffler, U. Lhose, Ch. Peuker, O. Oehlmann, L.M. Kustov, V.L. Zholobenko and V.B. Kazansky, Zeolites 10 (1990) 266.
[15] P.A. Jacobs and W.J. Mortier, Zeolites 2 (1982) 226.
[16] A. Janin, M. Maache, J.C. Lavalley, J.F. Joly, F. Raatz and N. Szydlowski, Zeolites 11 (1991) 391.
[17] Z. Macedo, PhD Thesis, University Paris VI, Paris, France (1988).
[18] J. Weitkamp, S. Ernst and R. Kumar, Appl. Catal. 27 (1986) 207.
[19] J.A. Martens, M. Tielen, P.A. Jacobs and J. Weitkamp, Zeolites 4 (1984) 98.